

# Final Technical Report

## High Surface Area Electrode Research

Supported under Grant #N00014-96-1-1109  
Office of the Chief of Naval Research  
Report for the period 7/10/96-12/31/96

S. Roberson and R. F. Davis  
North Carolina State University  
Materials Science and Engineering Department  
Campus Box 7907  
Raleigh, NC 27695

### DISTRIBUTION STATEMENT A

Approved for public release;  
Distribution Unlimited

December, 1996

19970106 078

DTIC QUALITY INSPECTED 1

REPORT DOCUMENTATION PAGE			Form Approved OMB No. 0704-0188	
Public reporting burden for this collection of information is estimated to average 1 hour per response, including the time for reviewing instructions, searching existing data sources, gathering and maintaining the data needed, and completing and reviewing the collection of information. Send comments regarding this burden estimate or any other aspect of this collection of information, including suggestions for reducing this burden to Washington Headquarters Services, Directorate for Information Operations and Reports, 1215 Jefferson Davis Highway, Suite 1204, Arlington, VA 22202-4302, and to the Office of Management and Budget Paperwork Reduction Project (0704-0188), Washington, DC 20503.				
1. AGENCY USE ONLY (Leave blank)	2. REPORT DATE December, 1996	3. REPORT TYPE AND DATES COVERED Final Technical 7/10/96-12/31/96		
4. TITLE AND SUBTITLE High Surface Area Electrode Research		5. FUNDING NUMBERS 96PR06926-00 312 N68892 N66020 4B855		
6. AUTHOR(S) Robert F. Davis				
7. PERFORMING ORGANIZATION NAME(S) AND ADDRESS(ES) North Carolina State University Hillsborough Street Raleigh, NC 27695		8. PERFORMING ORGANIZATION REPORT NUMBER N00014-96-1-1109		
9. SPONSORING/MONITORING AGENCY NAMES(S) AND ADDRESS(ES) Sponsoring: ONR, Code 312, 800 N. Quincy, Arlington, VA 22217-5660 Monitoring: Admin. Contracting Officer, ONR, Regional Office Atlanta 101 Marietta Tower, Suite 2805 101 Marietta Street Atlanta, GA 30323-0008		10. SPONSORING/MONITORING AGENCY REPORT NUMBER		
11. SUPPLEMENTARY NOTES				
12a. DISTRIBUTION/AVAILABILITY STATEMENT Approved for Public Release; Distribution Unlimited		12b. DISTRIBUTION CODE		
13. ABSTRACT (Maximum 200 words)  Molybdenum nitride ( $\text{Mo}_x\text{N}$ ( $x=1$ or $2$ )) films, $15\text{ }\mu\text{m}$ thick, have been deposited via chemical vapor deposition (CVD) on $50\text{ }\mu\text{m}$ thick polycrystalline titanium substrates using molybdenum pentachloride ( $\text{MoCl}_5$ ) and $\text{NH}_3$ in a cold wall reactor with vertical pancake heaters. The surface morphology of the films was slightly porous but did not contain the large cracks typical of high surface area $\text{Mo}_x\text{N}$ films prepared by conversion of $\text{MoO}_3$ . Debye-Scherrer calculations indicate that the average particle size of the films was approximately $50\text{ nm}$ . The CVD $\text{Mo}_x\text{N}$ films had a two-phase structure which appeared to be 60% d-MoN and 40% g-Mo <sub>2</sub> N. Energy dispersive X-ray (EDX) data did not reveal the presence of oxygen and chlorine in films deposited above $600^\circ\text{C}$ . Electrode evaluation via AC impedance spectroscopy and cyclic voltammetry indicates that CVD films were capacitive with a voltage stability of 0.9 volts in 6.4 M KOH.				
14. SUBJECT TERMS molybdenum nitride, films, chemical vapor deposition, molybdenum pentachloride, ammonia, surface morphology, particle size, energy dispersive X-ray, oxygen chlorine, AC impedance spectroscopy, cyclic voltammetry, voltage stability			15. NUMBER OF PAGES 9	
			16. PRICE CODE	
17. SECURITY CLASSIFICATION OF REPORT UNCLAS	18. SECURITY CLASSIFICATION OF THIS PAGE UNCLAS	19. SECURITY CLASSIFICATION OF ABSTRACT UNCLAS	20. LIMITATION OF ABSTRACT SAR	

# Characteristics of Molybdenum Nitride Electrodes Grown Via Chemical Vapor Deposition

Molybdenum nitride ( $\text{Mo}_x\text{N}$  ( $x=1$  or  $2$ )) films,  $15\text{ }\mu\text{m}$  thick, have been deposited via chemical vapor deposition (CVD) on  $50\text{ }\mu\text{m}$  thick polycrystalline titanium substrates using molybdenum pentachloride ( $\text{MoCl}_5$ ) and  $\text{NH}_3$  in a cold wall reactor with vertical pancake heaters. The surface morphology of the films was slightly porous but did not contain the large cracks typical of high surface area  $\text{Mo}_x\text{N}$  films prepared by conversion of  $\text{MoO}_3$ . Debye-Scherrer calculations indicate that the average particle size of the films was approximately  $50\text{ nm}$ . The CVD  $\text{Mo}_x\text{N}$  films had a two-phase structure which appeared to be  $60\%$   $\delta\text{-MoN}$  and  $40\%$   $\gamma\text{-Mo}_2\text{N}$ . Energy dispersive X-ray (EDX) data did not reveal the presence of oxygen and chlorine in films deposited above  $600^\circ\text{C}$ . Electrode evaluation via AC impedance spectroscopy and cyclic voltammetry indicates that CVD films were capacitive with a voltage stability of  $0.9\text{ volts}$  in  $6.4\text{ M KOH}$ .

## I. Introduction

The numerous potential applications of conductive high surface area (HSA) materials have prompted research and development into growth of these materials. At present, either HSA graphite powder or ruthenium oxide is generally used as electrode materials for double layer capacitors. However, outgassing of  $\text{CO}$  in aqueous electrolytes during cyclic charging and discharging limits the use of the former and the latter is uneconomical. Due to these problems, alternative materials are being investigated for use as double layer capacitor electrodes as substitutes for graphite and ruthenium oxide. Alternative candidate materials include the transition metal nitrides  $\text{M}_x\text{N}_y$  ( $\text{M} = \text{Mo}, \text{Ti}, \text{Ni}, \text{V}, \text{Cr}, \text{or W}$ ), which have been shown to have electrical conductivities exceeding  $10^4\text{ ohm}^{-1}\text{cm}^{-1}$  and good resistance to electrochemical decomposition in aqueous electrolytes [1]. More specifically due to its high electrical conductivity and resistance to electrochemical decomposition, molybdenum nitride is a promising candidate electrode material. However, to form high surface area films ( $> 30\text{ m}^2/\text{g}$ ) of molybdenum nitride, it is advantageous to make use of densification via conversion of  $\text{MoO}_3$  to molybdenum nitride [2-5]. Within the molybdenum compound family, the bulk density of  $\text{MoO}_3$  ( $\rho = 4.69\text{ g/cm}^3$ ) is less than  $\text{MoN}$  ( $\rho = 9.05\text{ g/cm}^3$ ), and  $\text{Mo}_2\text{N}$  ( $\rho = 9.50\text{ g/cm}^3$ ). In the conversion of  $\text{MoO}_3$  to molybdenum nitride, it is evident that the formation  $\text{Mo}_2\text{N}$  or  $\text{MoN}$  would cause a large increase in surface area (i.e., microcracks, pores, and cavitation) given that the densification is not associated with significant shrinkage of the nitride.

Upon trying to convert  $\text{MoO}_3$  films to  $\text{Mo}_x\text{N}$  some unreacted oxides will remain [6]. Molybdenum dioxide ( $\text{MoO}_2$ ), which is produced in the incomplete conversion of  $\text{MoO}_3$  to  $\text{Mo}_x\text{N}$ , has a + 0.676 volt stability in 4.4 M  $\text{H}_2\text{SO}_4$  electrolyte. Such oxide contaminated  $\text{Mo}_x\text{N}$  electrodes are limited to a 0.70 volt stability in charging and discharging cycles in 4.4 M  $\text{H}_2\text{SO}_4$  electrolytes. To reduce the oxide contamination in  $\text{Mo}_x\text{N}$  electrodes, a direct growth process (CVD) using  $\text{MoCl}_5$  and  $\text{NH}_3$  has been employed.

## II. Experimental Procedures

As-received polycrystalline titanium substrates were cut into 1" squares and degreased in pure trichloroethylene, acetone, and methanol in sequential order. The substrates were then etched in a solution of 1.0 M  $\text{HCl}$  at  $90^\circ\text{C}$  for 10 minutes to remove the oxide scale layer. The etched substrates were rinsed and held in pure methanol prior to deposition.

The etched substrates were placed on a molybdenum holder contained in a cold wall, vertical CVD system. The system was evacuated to  $10^{-3}$  Torr and back-filled with ultra high purity (UHP)  $\text{N}_2$  to 1000 Torr. This process was repeated seven times to reduce oxygen present in the system to the amount contained in the UHP  $\text{N}_2$ . The UHP  $\text{N}_2$  was also used as the carrier gas for the  $\text{MoCl}_5$ , which was contained in a stainless steel metalorganic bubbler. The bubbler was maintained at a constant temperature of  $55^\circ\text{C}$  to give a  $\text{MoCl}_5$  vapor pressure of 2 Torr. The  $\text{MoCl}_5/\text{N}_2$  gas delivery line to the deposition region was heated to slightly higher temperatures than the bubbler temperature to reduce condensation of  $\text{MoCl}_5$ . The unheated  $\text{NH}_3$  gas delivery line was isolated from the  $\text{MoCl}_5$  delivery line to minimize the formation of  $\text{NH}_4\text{Cl}$ . The formation of  $\text{NH}_4\text{Cl}$  was also minimized by employing an alternating cycle deposition method, in which  $\text{MoCl}_5$  was cycled for 0.5 seconds every minute, while  $\text{NH}_3$  flow was maintained at all times except when the  $\text{MoCl}_5/\text{N}_2$  was flowing. The  $\text{MoCl}_5/\text{N}_2$  and  $\text{NH}_3$  flow rates during the deposition process were 2.5 l/min and 1.5 l/min respectively, and were controlled by mass flow controllers. The deposition pressure was 100 Torr and was maintained by a throttle valve. The substrates were heated by a resistive SiC-coated graphite heater to the desired  $\text{Mo}_x\text{N}$  deposition temperature, and the deposition cycle was initiated by flowing  $\text{N}_2/\text{MoCl}_5$  for 0.5 seconds. Termination of the deposition process was accomplished by cessation of the  $\text{MoCl}_5/\text{N}_2$  flow, while maintaining  $\text{NH}_3$  flow for 5 minutes at deposition temperatures.

The electrical, structural, and chemical characteristics of the  $\text{Mo}_x\text{N}$  films were analyzed. Scanning electron microscopy (SEM) was performed using a JEOL 6400FE operating at 5 kv which was equipped with an Oxford Light Element Energy Dispersive X-ray (EDX) Microanalyzer. X-ray diffraction (XRD) data was obtained on a Rigaku X-ray diffraction apparatus operating at 27.5 kv. Electrical properties of the  $\text{Mo}_x\text{N}$  electrodes were evaluated by AC impedance spectroscopy and cyclic voltammetry in 6.4M  $\text{KOH}$  electrolytes.

### III. Results and Discussion

The HSA film electrodes currently used in double layer energy storage devices generally have a macroscopic, highly-cracked microstructure. In the present research, polycrystalline  $\text{Mo}_x\text{N}$  films have been deposited on titanium substrates without the mud-crack macrostructure. As shown in Fig. 1a, the thickness across the textured surface of CVD  $\text{Mo}_x\text{N}$  films varied by 1  $\mu\text{m}$  on 15  $\mu\text{m}$  thick films. An SEM micrograph of a  $\text{Mo}_x\text{N}$  electrode prepared by the conversion of  $\text{MoO}_3$  is shown for comparison in Fig. 1b. The surface roughness of CVD  $\text{Mo}_x\text{N}$  films is more apparent in 45° rotation SEM micrographs shown in Fig. 2a and Fig. 2b. The surface roughness is believed to be due to a combination of high deposition rates (1  $\mu\text{m}/\text{min}$ ) and rapid surface reaction of  $\text{MoCl}_5$  and  $\text{NH}_3$ . With a deposition rate of 1  $\mu\text{m}/\text{min}$  at 600°C, very little surface diffusion occurs and particles remain “frozen” on the surface and react rapidly when exposed to  $\text{NH}_3$ . Higher deposition rates would be detrimental to film quality, crystallinity, and adhesion.

The chemical properties of the  $\text{Mo}_x\text{N}$  films were examined using XRD and EDX. X-ray diffraction patterns of the two phase CVD and converted  $\text{Mo}_x\text{N}$  films are shown in Fig. 3a and Fig. 3b, respectively. The CVD films consisted of  $\approx 60\%$   $\delta$ - $\text{MoN}$  and 40%  $\gamma$ - $\text{Mo}_2\text{N}$ ; and converted  $\text{Mo}_x\text{N}$  films consisted of  $\approx 60\%$   $\gamma$ - $\text{Mo}_2\text{N}$  and 40%  $\delta$ - $\text{MoN}$ . The peak broadening in the XRD patterns was due to nanoparticle formation in the films. Furthermore, the EDX pattern, with the nitrogen peak removed for clarity, of a typical CVD  $\text{Mo}_x\text{N}$  film deposited at 600°C indicates that no residual chlorides or oxides were present. However, at deposition temperatures less than 400°C chlorine was detected. This was due to the difficulty in thermally cracking  $\text{NH}_3$  at temperatures below 500°C. As shown in Fig. 4b, the EDX pattern for a typical  $\text{Mo}_x\text{N}$  film prepared by the conversion of  $\text{MoO}_3$  shows considerable amounts of oxygen present in the film. The oxygen present in the CVD  $\text{Mo}_x\text{N}$  films approximates the amount of residual oxygen present due to physical absorption of water, air, and hydrocarbons on the surface of the film.

The Debye-Scherrer equation (Eq. 1) was used to calculate the average particle size of the films using the XRD patterns,

$$d = K\lambda / \beta_{hkl} \cos\theta. \quad (1)$$

Theta ( $\theta$ ) is the Bragg angle;  $\lambda$  is the X-ray wavelength;  $\beta_{hkl}$  is the peak width at half maximum peak height, corrected for instrument broadening; and the correction factor  $K$  was taken as unity. To minimize the effects of peak broadening due to residual stresses, particle size calculations were conducted using peak values less than 20°. As shown in Table I, the average particle size of the CVD  $\text{Mo}_x\text{N}$  films was 53 nm, where as the average particle size of converted  $\text{Mo}_x\text{N}$  films was 10 nm.

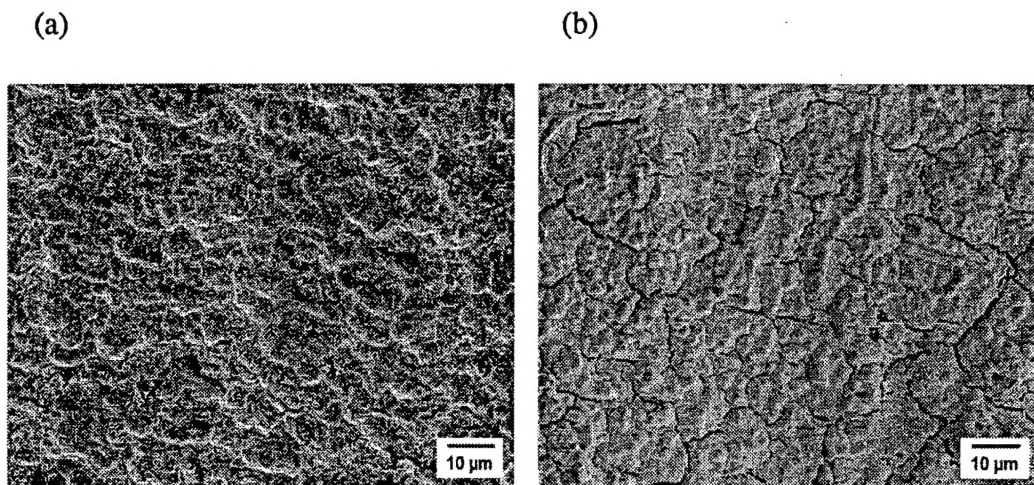


Figure 1. SEM micrographs of (a) CVD  $\text{Mo}_x\text{N}$  film and (b)  $\text{Mo}_x\text{N}$  film converted from  $\text{MoO}_3$ . The surface of the CVD film does not have the mud crack structure present in (b).

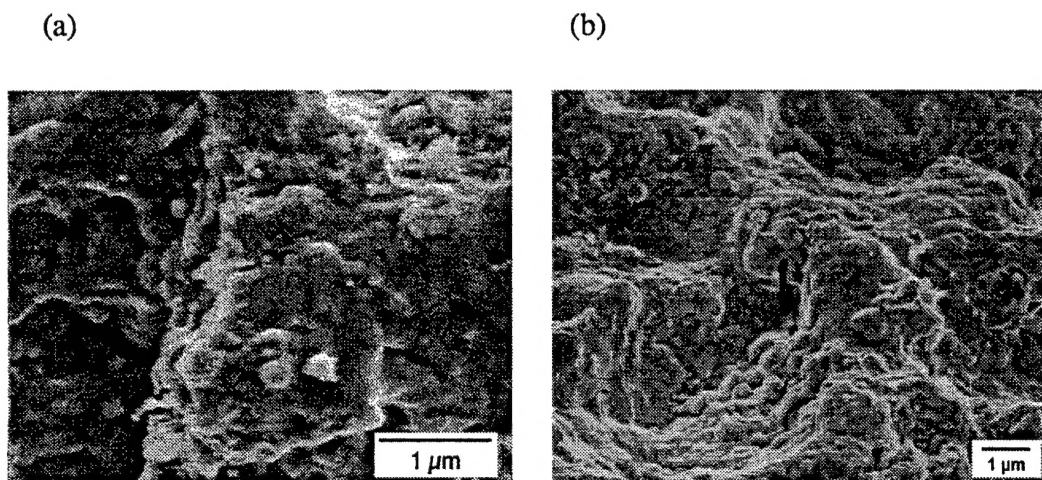


Figure 2. Scanning electron micrographs of CVD  $\text{Mo}_x\text{N}$  films at  $45^\circ$  rotation at (a) magnification of 25,000 and (b) magnification of 10,000. Note the variation in film thickness and the roughness of the surface.

Surface area generation in the conversion of  $\text{MoO}_3$  to  $\text{Mo}_x\text{N}$  is the result of the densification of  $\text{MoO}_3$  to  $\text{Mo}_2\text{N}$  without the collapse of individual particles. This is called “topotactic” because the crystallographic direction relationships between  $\text{MoO}_3$  and  $\text{Mo}_2\text{N}$  are retained [5]. The topotactic reaction creates surface area by the generation of pores in  $\text{Mo}_2\text{N}$  without the collapse of individual crystals. For CVD  $\text{Mo}_x\text{N}$  films, surface area generation takes place by a different process. Molybdenum pentachloride (trigonal,  $\rho = 2.98 \text{ g/cm}^3$ ) reacts rapidly with  $\text{NH}_3$  at elevated temperatures to produce  $\text{Mo}_x\text{N}$  ( $\rho = 9.05 \text{ g/cm}^3$ ). This change in density, can create adherence problems. However, the



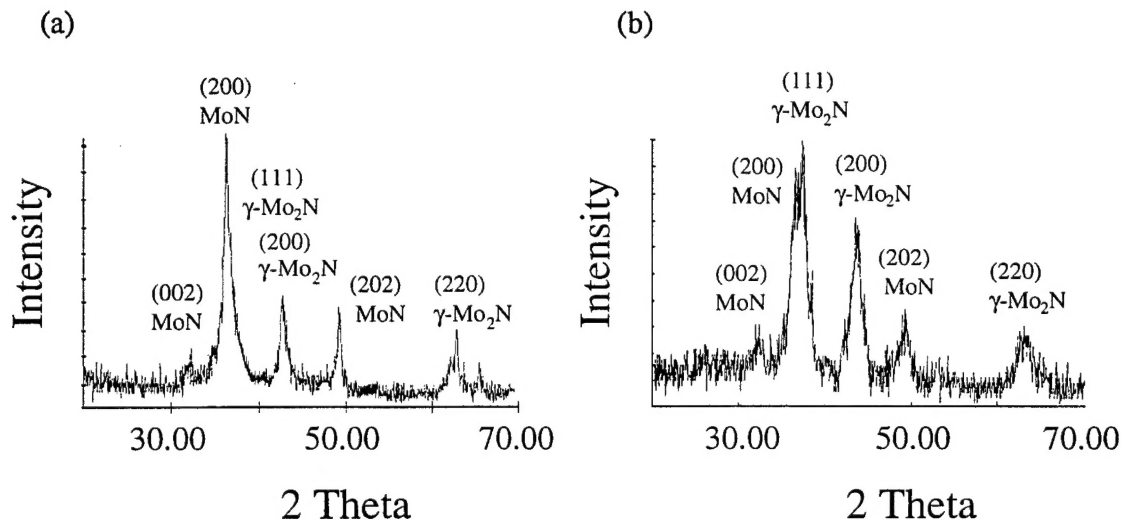


Figure 3. X-ray diffraction patterns of (a) CVD  $\text{Mo}_x\text{N}$  film and (b)  $\text{Mo}_x\text{N}$  film converted from  $\text{MoO}_3$ . The peak broadening in (a) and (b) is due to nanoparticle formation.

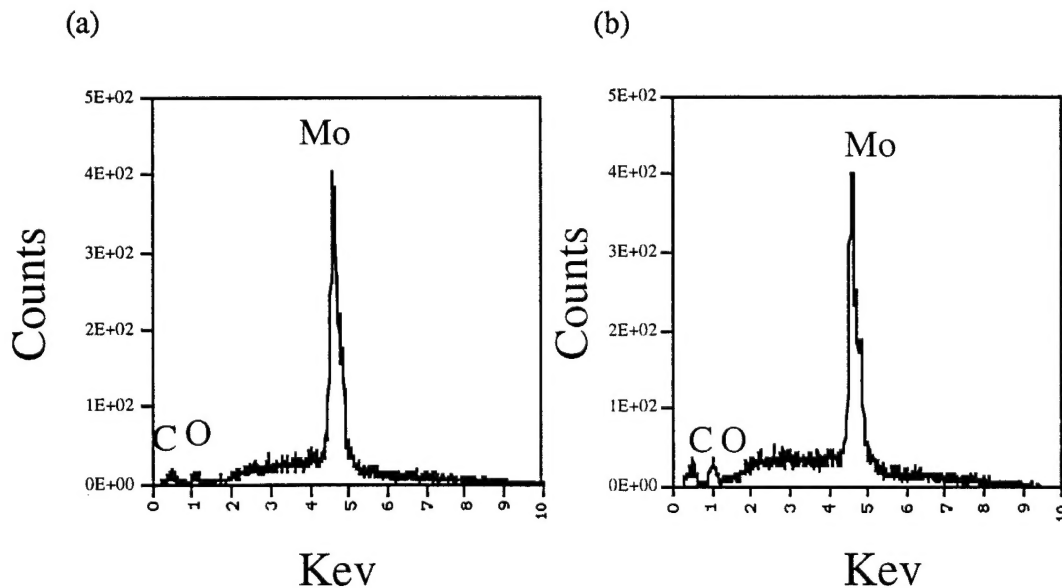


Figure 4. Energy dispersive X-ray patterns of (a) CVD  $\text{Mo}_x\text{N}$  film and (b)  $\text{Mo}_x\text{N}$  film converted from  $\text{MoO}_3$ . Oxygen contamination was observed in (b).

rapid reaction of  $\text{MoCl}_5$  and  $\text{NH}_3$  can produce a porous structure without sacrificing film adherence if the deposition reaction is optimized. If the deposition rate is too slow, the complete densification of  $\text{MoCl}_5$  will occur which can reduce the surface area. However, if the deposition rate is optimal, then the densification of  $\text{MoCl}_5$  to  $\text{Mo}_x\text{N}$  occurs rapidly to

Table I. Calculated Average Particle Sizes of  $\text{Mo}_x\text{N}$  Films Produced by CVD and Conversion Form  $\text{MoO}_3$

Process	Phase	$\theta$	$\cos \theta$	$\beta_{hkl}$	Particle Size
CVD	MoN	15.944	0.9615	0.0030	53.31 nm
CVD	MoN	18.103	0.9504	0.0030	54.09 nm
CVD	$\text{Mo}_2\text{N}$	18.688	0.9472	0.0031	51.72 nm
Conversion	MoN	15.944	0.9615	0.0147	10.47 nm
Conversion	MoN	18.103	0.9504	0.0149	10.33 nm
Conversion	$\text{Mo}_2\text{N}$	18.688	0.9472	0.0151	10.19 nm

produce pores in the bulk of the structure, while remaining adhered to the substrate. As shown in Fig. 5a, the increase in deposition rate produced an increase in the surface area of the films. This is a direct result of the rapid reaction of  $\text{MoCl}_5$  and  $\text{NH}_3$ . The surface area was also discovered to increase with the deposition temperature, as shown in Fig. 5b. This was due to the complete conversion of  $\text{MoCl}_5$  to  $\text{Mo}_x\text{N}$  and subsequent production of pores in the film.

Molybdenum nitride electrodes were evaluated in 6.4M KOH electrolytes by AC impedance spectroscopy and cyclic voltammetry to determine their capacitance and electrochemical stability. In Fig. 6, the slope of the line in plots of frequency versus impedance is -1 which is typical of ideal porous electrodes displaying double layer capacitance. In Fig. 7, a cyclic voltammogram of a representative CVD  $\text{Mo}_x\text{N}$  electrode in the 6.4M KOH electrolyte is shown. The capacitance was determined to be  $0.30 \text{ F/cm}^2$ , which is less than  $\text{Mo}_x\text{N}$  electrodes prepared by conversion of  $\text{MoO}_3$ . However, the voltage stability of CVD  $\text{Mo}_x\text{N}$  electrodes is 0.9 volts which is 0.2 volts higher than  $\text{Mo}_x\text{N}$  electrodes prepared by the conversion of  $\text{MoO}_3$ .

#### IV. Conclusions

$\text{Mo}_x\text{N}$  (MoN 60% and  $\text{Mo}_2\text{N}$  40%) films void of large cracks on the surface have been deposited via CVD on polycrystalline titanium substrates. The EDX data shows a significant reduction in oxygen contamination in  $\text{Mo}_x\text{N}$  CVD films when compared to  $\text{Mo}_x\text{N}$  films prepared by the conversion of  $\text{MoO}_3$ . The average particle size of the CVD films was determined by Debye-Scherrer calculations to be  $\approx 50 \text{ nm}$ . The two phase  $\text{Mo}_x\text{N}$  films consisted of  $\approx 60\%$  MoN and  $40\% \gamma\text{-Mo}_2\text{N}$ . AC Impedance and cyclic voltammetry data indicate that CVD  $\text{Mo}_x\text{N}$  films are capacitive with voltage stability of 0.9 volts in 6.4 M KOH electrolytes.



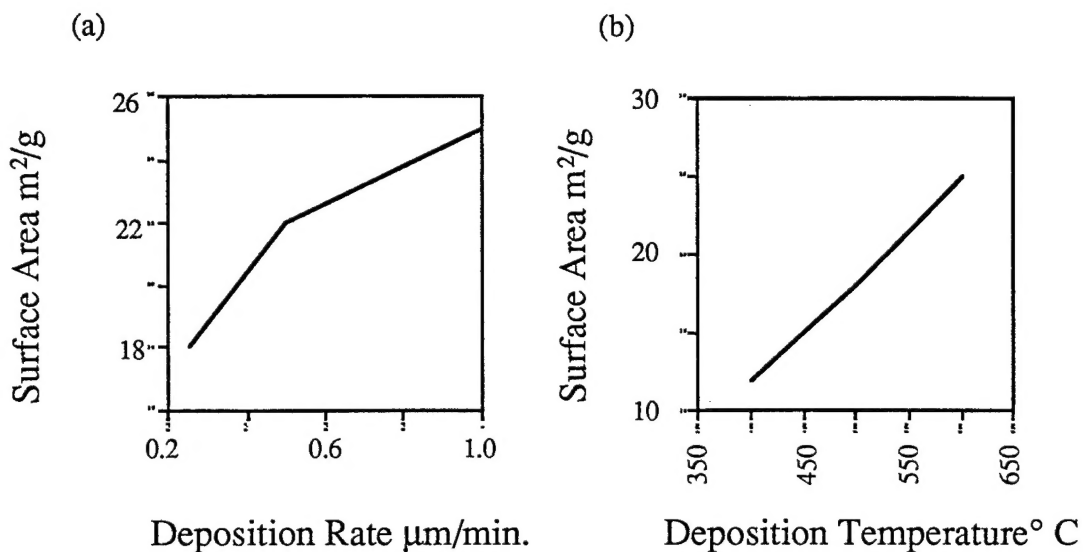


Figure 5. Plots of the surface area of CVD  $\text{Mo}_x\text{N}$  films versus (a) deposition rate at  $600^{\circ}\text{C}$  and (b) deposition temperature. The surface area was found to increase with both increasing deposition temperature and deposition rate.

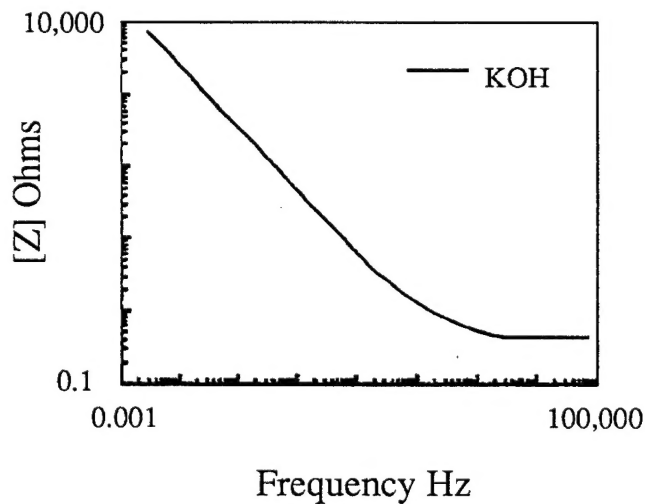


Figure 6. An AC impedance spectroscopy plot of frequency versus impedance. The slope of the line indicates a capacitive response of the electrode.

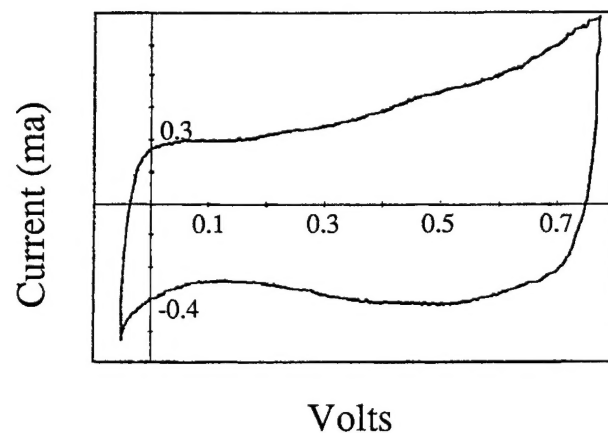


Figure 7. Cyclic voltammogram of CVD  $\text{Mo}_x\text{N}$  electrode in 6.4 M KOH.

#### V. References

1. S. L. Roberson, D. Finello and R. F. Davis, MRS Soc. Symp. Proc., Fall 1996, (to be published in Symp. P Proc.).
2. J. G. Choi, R. L. Curl and L. T. Thompson, Journal of Catalysis **146**, 218 (1994).
3. R. S. Wise and E. J. Markel, Journal of Catalysis **145**, 344 (1994).
4. L. Volpe and M. Boudart, Journal of Solid State Chemistry **59**, 332 (1985).
5. C. H. Jagers, J. M. Michaels and A. M. Stacy, Chemistry of Materials **2**, 150 (1990).
6. S. L. Roberson, D. Finello and R. F. Davis, MRS Soc. Symp. Proc., Fall 1996, (to be published in Symp. V Proc.).

## Distribution List

Dr. Alvin M. Goodman Office of Naval Research Electronics Division, Code: 312 Ballston Tower One 800 N. Quincy Street Arlington, VA 22217-5660	3
Administrative Contracting Officer Office of Naval Research Regional Office Atlanta 101 Marietta Tower, Suite 2805 101 Marietta Street Atlanta, GA 30323-0008	1
Director, Naval Research Laboratory ATTN: Code 2627 Washington, DC 20375	1
Defense Technical Information Center 8725 John J. Kingman Road, Suite 0944 Ft. Belvoir, VA 22060-6218	2